Suppression of Zeroth-Order Diffraction in Phase-Only Spatial Light Modulator via Destructive Interference with a Correction Beam

Wynn Dunn Gil D. Improso, Giovanni A. Tapang and Caesar A. Saloma
National Institute of Physics, University of the Philippines, Diliman, Quezon City, Philippines

Keywords: 42.30.Kq Fourier Optics, 42.30.Lr Modulation and Optical Transfer Functions, 42.30.Rx Phase Retrieval, 42.40.Jv Computer Generated Holograms.

Abstract: We suppress the unwanted zeroth order diffraction (ZOD) contributed by the dead areas of a spatial light modulator with a correction beam that is independently created from the desired target. We use the Gerchberg-Saxton algorithm to generate the phase of the correction beam profile that would match correctly with that of the ZOD. The correction beam intensity is regulated using a coefficient to match also with that of the ZOD. Numerical simulation reveals a ZOD suppression that is as high as -99% but only -32% has been achieved so far experimentally.

1 INTRODUCTION

The increasing capability to manipulate the properties of light accurately and reliably has opened many interesting practical possibilities in optics in the past decade and a half (Eriksen et al, 2002; Polin et al, 2005; Palima and Daria 2007; Nikolenko et al, 2008; Jenness et al, 2010; Hilario et al, 2014). Complicated light intensity distributions could be realized by manipulating the phase or the amplitude, or both. Most applications have employed the more efficient phase-only modulation where light loss (from spatial filtering) is minimal (Zhu and Wang 2014). In phase modulation, light is tailored through the use of phase objects such as lenses, prisms, and recently, the spatial light modulator (SLM).

The SLM allows for the full control of the spatial phase profile of the propagating beam. The desired phase distribution is imposed pixel by pixel to the incident light using a computer generated hologram (CGH) that serves as the input to the SLM (Eriksen et al, 2002). Because of its versatility, the SLM has been widely used in diverse applications such as optical trapping (Dufresne 2001; Melville 2003), microfabrication (Jenness et al, 2010; Farsari et al, 1999), microscopy (Shao et al, 2012; Fahrbach et al, 2013) and astronomy (Alagao et al, 2016).

In between two adjacent pixels of an SLM is a non-functional (dead) area, the size of which is described by the fill factor F. The light that hits these dead areas are not modulated by the SLM, and hence results to a zero order diffraction beam (ZOD) at the optical axis in the Fourier plane (Palima and Daria 2007). The ZOD introduces a high intensity illumination that distorts the desired light profile and undermines the reconstruction quality.

A commonly used solution to bypass the dire effects of the ZOD is to shift the light pattern away from the optical axis. This technique limits the size of the functional area and reduces diffraction efficiency. Another approach is to place in an intermediate plane a physical beam block that fully removes the ZOD (Polin et al, 2005). This results in a non-accessible region in the final reconstruction since any part of the desired pattern that is near the ZOD location of the ZOD would also be affected. Daria and Palima (2007) proposed to create a correction beam with the same profile as that of the ZOD together with the desired target. Destructive interference is induced between the correction beam and the ZOD by forcing a π-phase difference resulting in a suppressed ZOD. However, the technique becomes slow in cases that involve different desired targets that require a set of unique CGH profiles. The ZOD and the corresponding correction beam profile also have to be precisely matched thereby lengthening the CGH calculation time.

In this paper, we suppress the ZOD with a correction beam that is generated via the SLM without a physical

Improso W., Tapang G. and Saloma C.
Suppression of Zeroth-Order Diffraction in Phase-Only Spatial Light Modulator via Destructive Interference with a Correction Beam.
DOI: 10.5220/0006129802080214
In *Proceedings of the 5th International Conference on Photonics, Optics and Laser Technology (PHOTOPTICS 2017)*, pages 208-214
ISBN: 978-989-758-223-3

block or a grating. The required phase profile for the correction beam is independently calculated from the desired light configuration. The final phase input to the SLM is described by the field addition method as discussed by Hilario et al. (2014).

We calculate the hologram input that contains the phase information needed for constructing the correction beam and the desired target. The holograms serve as inputs to the SLM. The technique is described and evaluated in the next Section.

2 FIELD ADDITION METHOD AND EXPERIMENTAL VERIFICATION

The SLM that is used is Hamamatsu PPM X8267, with $F = 0.8$. The SLM has a $20mm \times 20mm$ window corresponding to 768×768 pixel size.

2.1 Phase Calculation

For suppression to succeed at the Fourier plane, there must be full destructive interference between the unwanted ZOD and the correction beam, which is possible when their profiles are correctly matched - the total energies of the correction beam and the ZOD are equal and their phase difference is equal to π (destructive interference).

The phase needed to construct the correction beam $\phi_{corr}(\eta,\chi)$ where η and χ are the coordinates, is calculated using the Gerchberg-Saxton algorithm, a phase retrieval algorithm consisting of forward and inverse Fourier transforms. The constraint in the SLM and reconstruction plane is the aperture and the ZOD amplitude distribution, respectively. The correction beam will then have a similar profile to the ZOD

The ZOD amplitude distribution is obtained by simulating the field caused by the dead areas of the SLM as described by the fill factor. The aperture of the SLM is oversampled 400 times, meaning each pixel is sampled to 20×20. Thus the 768×768 SLM will be oversampled to 15360×15360. The outer pixels of each 20×20 pixel is imposed to have zero phase shift to simulate the non-modulating dead areas. The field caused by these non-modulating areas is then separated and propagated using Fourier transform to obtain the ZOD amplitude distribution. The middle 768×768 of the reconstruction is the ZOD amplitude. This is shown in Figure 1.

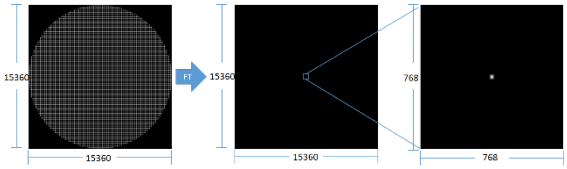

Figure 1: The calculation for ZOD target.

The phase to construct a desired target, $\phi_{target}(\eta,\chi)$, is also calculated. The desired target represents the application that will be done using the SLM. In this work, the change in the ZOD intensity is measured and therefore the target must not have any intensity near the ZOD.

The fields due to $\phi_{corr}(\eta,\chi)$ and $\phi_{target}(\eta,\chi)$ are then given by:

$$U_{corr}(\eta,\chi) = A(\eta,\chi)e^{i\phi_{corr}(\eta,\chi)} \quad (1)$$

$$U_{target}(\eta,\chi) = A(\eta,\chi)e^{i\phi_{target}(\eta,\chi)} \quad (2)$$

where $A(\eta,\chi)$ is the amplitude at the aperture of the SLM. The phase input to the SLM, $\phi_{slm}(\eta,\chi)$ is then given by:

$$\phi_{slm}(\eta,\chi) = \mathrm{Arg}\{c_{corr}U_{corr} + c_{target}U_{target}\} + \phi_{shift} \quad (3)$$

where Arg function gives the phase, ϕ_{shift} the constant phase added to induce destructive interference between ZOD and correction beam, and c_{corr} and c_{target} are constants multiplied to U_{corr} and U_{target}, respectively. The constants are used to control the amount of light used to reconstruct the correction beam and target, and has the following constraint:

$$c_{corr} + c_{target} = 1 \quad (4)$$

Coefficients c_{corr} and c_{target} are scanned from zero to 1. If c_{corr} is greater than c_{target}, this means that the correction beam has higher total light intensity than the target. The best result is when ZOD is suppressed at low values of c_{corr} since this means that more energy is used to create the desired target. ϕ_{shift}, is scanned from 0 to 2π in increments. It is assumed that the dead areas impose constant phase shift over the whole SLM aperture and thus we need to obtain the correct phase shift so that destructive interference occurs between the ZOD and correction beam.

The calculation of ϕ_{slm} is shown in Figure 2. ϕ_{slm} is converted to 8-bit images using the phase response of the SLM.

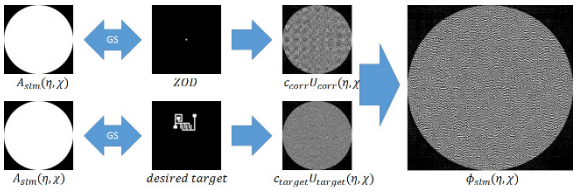

Figure 2: Calculation for the phase input SLM, $\phi_{slm}(\eta, \chi)$.

2.2 Optical Implementation

Light hits M1 and then a half-wave plate that ensures a correct polarization of the incident light to the SLM (see Figure 3). It is then directed to 10 × expander set-up by M2. The expander set-up is composed of L1 and L2 ($f = 10mm$ and $f = 100mm$, respectively). This expands the beam 10× to fill the back aperture of the objective lens (OL, 4 ×, $NA = 0.16$). At the focus, a pinhole (PH, $r = 25\mu m$) is placed to spatially filter the light. L3 ($f = 300mm$) is positioned 300mm from the PH. The output is a collimated plane wave directed to the SLM ($F = 0.8, 20mm \times 20mm$) using a beam splitter (BS). Hologram is inputted to the SLM using a computer. Light that is reflected from the SLM then is focused by L4 ($f = 300mm$) to a camera. Neutral density filters (NDF) are placed before L4 to control the intensity of light that hits CCD ($6.40mm \times 4.80mm$, $640\ pixels \times 480\ pixels$) and avoid light saturation. The images from the CCD are captured by computer (not shown).

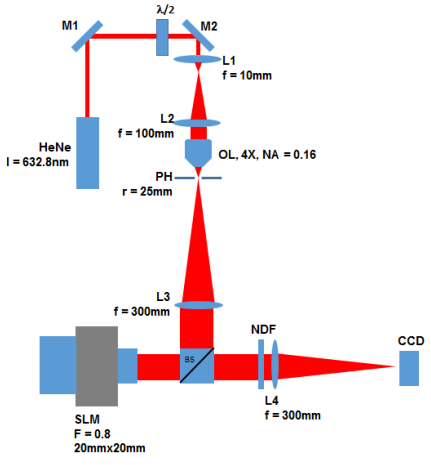

Figure 3: The optical set-up.

The initial ZOD value is determined with a hologram that reconstructs the desired target only in the experiment. NDFs are added or subtracted to avoid saturating the camera. The image is then captured and the original ZOD intensity is obtained by summing the total intensities around the ZOD area to yield the I_{ZOD} information. The computed phase is then inputted to the SLM. We used 33 values of c_{corr} from 0 to 1. For each c_{corr} value, the phase shift ranges from 0 to 2π. For each phase input, we obtain the I_{method}. Which is given by total ZOD intensity at a constant NDF value. The relative intensity R is then calculated using the following equation:

$$R = \frac{I_{method} - I_{ZOD}}{I_{ZOD}} \times 100\% \quad (5)$$

where R > zero means a decrease in ZOD intensity indicating either a constructive interference between the correction beam and the ZOD, or a total correction beam energy that is overshooting that of the ZOD. Even when the destructive interference is total, sufficient energy can still remain in the correction beam to create another ZOD. A value of $R = 0$ indicates that nothing has changed while $R < 0$ implies a decrease in the total ZOD intensity. The ideal suppression result is: $I_{method} = 0$ or $R = -100\%$.

3 RESULTS AND DISCUSSIONS

3.1 Experimental Results

Figure 4 illustrates the dependence of R with ϕ_{shift} for different values of c_{corr}. The minimum R value is located at $\phi_{shift} = 0, 2\pi$. Linear behaviour happens when $c_{corr} \sim 1$ due to saturation in the camera. When constructive interference happens, the highest possible intensity can saturate the camera.

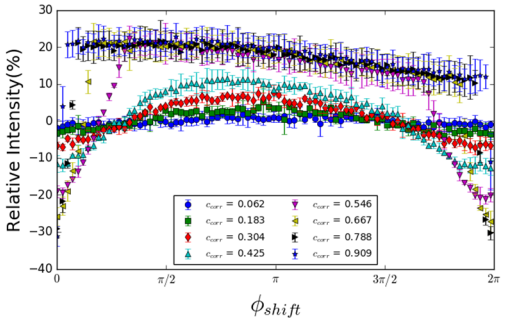

Figure 4: Relative intensity R vs. ϕ_{shift} for different c_{corr}.

For each c_{corr} value, the corresponding ZOD image is taken with the minimum R value (see Fig. 5). The total ZOD intensity is visually observed to gradually reduce as c_{corr} increases.

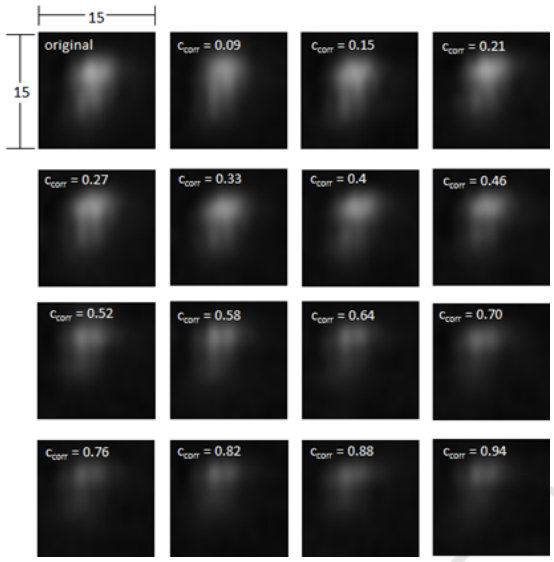

Figure 5: ZOD with lowest R per c_{corr} (frame size: 15^2 pixels).

Figure 6 plots the average minimum R for a given c_{corr} (three trials per point). The minimum R is steady for low c_{corr} values (up to c_{corr} equal to 0.3). The R value then decreases until c_{corr} = 0.82, where a ZOD suppression of -32% is achieved relative to its original value. It does not change significantly for $c_{corr} > 0.82$.

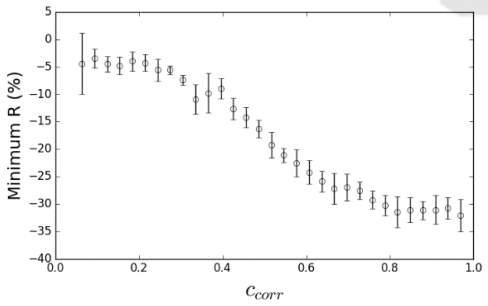

Figure 6: Average minimum R for a given c_{corr}.

3.2 Numerical Simulation

To describe the effects of ZOD suppression with a correction beam, we numerically model the performance of an SLM with a fill factor F of less than 1. We assume that only the dead areas affect the phase input and contribute to the ZOD intensity.

The simulation with $F < 1$ is performed by oversampling each hologram similar to the calculation of the ZOD (see Fig. 1). Oversampling is achieved by sampling each pixel at intervals that is much less than the pixel dimensions. In our case, each pixel is sampled 400 times (20×20 sampling points). To simulate the effect of the non-working (dead) areas, the outer pixels are assumed to have a zero phase shift contribution. We use a fill factor of F = 0.81.

First, we compare the correction beam profile with that of the ZOD. Propagating the field without the oversampling results to a reconstruction without the ZOD that produces only the desired target and the correction beam. The correction beam profile (S_{corr}) is compared to the ZOD (S_{ZOD}) using the Linfoot's criteria of method (Tapang and Saloma 2002). The following figures of merit are calculated: fidelity (F) which measures the overall similarity of two profiles: $F = 1 - \frac{<(S_{ZOD} - S_{corr})^2>}{<S_{ZOD}{}^2>}$; structural content ($C$) which measures the relative sharpness of peak profiles: $C = \frac{<S_{corr}{}^2>}{<S_{ZOD}{}^2>}$; and correlation quality (Q), which measures the alignment of peaks: $Q = \frac{<|S_{corr}||S_{ZOD}|>}{<S_{ZOD}{}^2>}$. F ranges from -1 to 1 and C and Q ranges from 0 to 1. If S_{corr} and S_{ZOD} are perfectly the same, we have $F = C = Q = 1$.

Next, we model the suppression of the ZOD by propagating the field with both the working areas and the dead areas. We Fourier transform the entire oversampled field that include the dead areas. Propagating the oversampled field results to a reconstruction with higher frequencies. We take the middle reconstruction, in the zeroth order, and consider the total ZOD intensity within a 40×40 square area to obtain the ZOD intensity without the desired target (see Fig. 7).

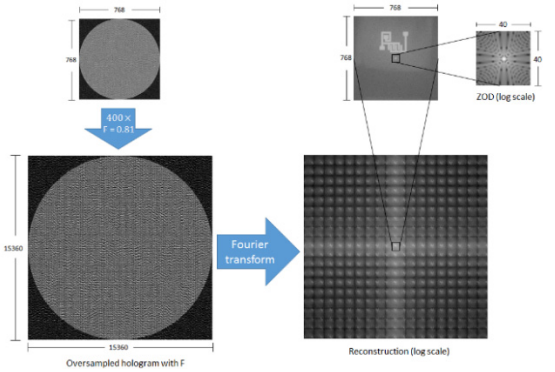

Figure 7: Simulating the effect of dead areas on the calculated hologram.

Figures 8a and 8b present the ZOD and the correction beam reconstructions for different c_{corr}, and the line profiles, respectively. Figure 8c presents the Linfoot's criteria of merit versus c_{corr}. The results show that the correction beam profile matches with that of the ZOD, to allow destructive interference to occur.

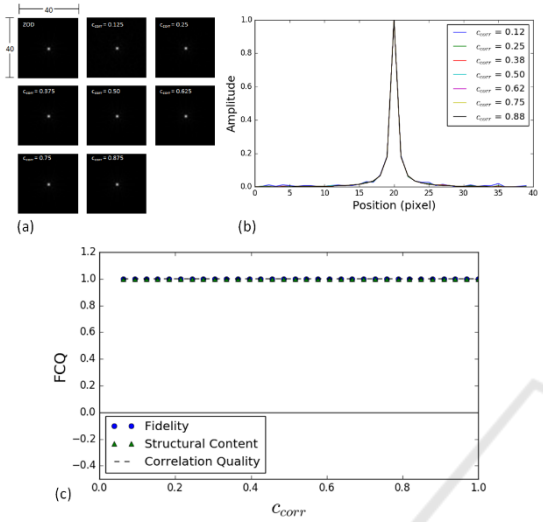

Figure 8: Comparison of ZOD and correction beam profiles. (a) ZOD reconstruction and correction beam reconstruction only. (b) Cross section profile of ZOD and the correction beam for different c_{corr}. (c) Linfoot's criteria of merit versus c_{corr}.

Figure 9 plots R versus ϕ_{shift} for different values of c_{corr}. The minimum R is found when ϕ_{shift} is equal to 0 and 2π, similar to the experimental result.

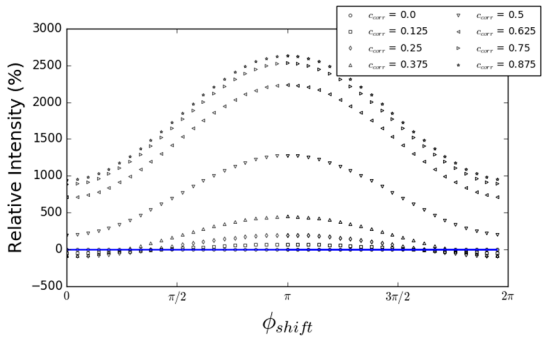

Figure 9: Relative intensity R versus ϕ_{shift}.

Finally, Fig. 10a presents sample images of the ZOD for different c_{corr}, while Fig. 10b plots minimum R versus c_{corr}. The minimum R plot reveals the possibility of -99% suppression at c_{corr} = 0.3125. A zero ZOD intensity is possible when the correction beam profile matches perfectly with that of the ZOD (see Fig. 8) and the remaining task is now matching the total energies of the two beams. The required total energy of the correction beam is obtained by tuning the c_{corr}, value.

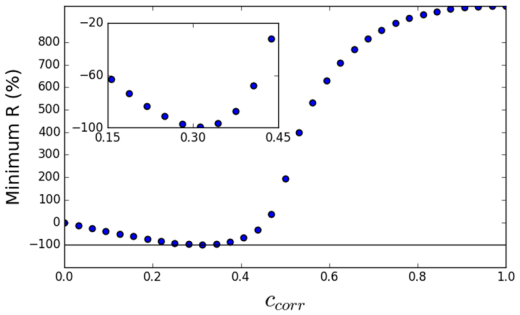

Figure 10: (a) The ZOD and the correction beam for different values of c_{corr}. (b) Minimum R versus c_{corr}. Inlet shows that minimum R reaches -99% at c_{corr} equals 0.3125.

Our experiments produce a degree of suppression that differs from the numerical prediction. The experimental results yield a negative value for the minimum R for all c_{corr}. As c_{corr} increases, the minimum R also decreases until c_{corr} = 0.82l. On the other hand, our simulation shows a decreasing minimum R only until c_{corr} = 0.3125. Second, the simulation predicts a 99% decrease in the ZOD intensity when c_{corr} = 0.3125 but only a 32% decrease is obtained experimentally and at c_{corr} = 0.82.

The difference between simulation and experimental results at low c_{corr} values (low suppression regime), may be attributed to a low correction beam energy that limits the degree of suppression. At high c_{corr}, values the discrepancy happens since in calculating for c_{corr} and in simulating the SLM, we have assumed that only the dead areas of the SLM contributed to ZOD generation. In practice there might be other sources that add to the total ZOD intensity that requires a higher correction beam energy (i.e. a larger c_{corr} value) for suppressing the ZOD. Other possible sources include imperfection in the anti-reflection coating (Sars et al, 2012), phase fluctuations (Lizana et al, 2008) and pixel crosstalk (Engstrom et al, 2012).

Other physical SLM limitations may also affect the profiles of the ZOD and the correction beam. They are unaccounted for in the simulation and produce additional mismatches between the ZOD and correction beam profiles and limits the strength of the destructive interference. The input hologram is also affected by spatial phase variations brought about by uneven illumination, imperfect flatness and pixel crosstalk which results to changes in the profile of the

correction beam, thereby further limiting the suppression that occurs.

4 CONCLUSIONS

The ZOD suppression has been demonstrated experimentally by inducing destructive interference between the ZOD and the correction beam. The correction beam is created with a desired target using the SLM. We have assumed that only the dead areas in the SLM contribute to the ZOD.

We calculate the fields necessary to create the desired target and correction beam separately, the input source to the GS algorithm being the aperture amplitude of the SLM. The final phase input to the SLM is obtained by calculating the phase of the sum of the two fields as described by Hilario et al. (2014). The energy directed to the correction beam is controlled using multiplicative constants c_{corr} and c_{target}.

The calculated holograms were inputted to the SLM, and the intensity of the ZOD was obtained from the captured images. We decreased the total intensity of the ZOD by 32% of its original value when c_{corr} is equal to 0.82.

We have simulated the potential of our technique and found a degree of a ZOD suppression that is as high as -99% of its original value which is possible if perfect similarity is achieved between the profiles of the ZOD and correction beam.

Differences in the numerical and experimental results may be attributed to other physical limitations of the real SLM that are unaccounted for in the numerical simulations. The said limitations alter the total ZOD intensity and require a different (higher) c_{corr} value for achieving the highest possible suppression. They can also alter the phase profiles of the ZOD and the correction beam with the dissimilarity limiting the degree of destructive interference that is realized. Possible misalignments of the optical elements may contribute to the profile differences as well as change the relative location of the ZOD and the correction beam. Addressing the abovementioned limitations would improve the degree of ZOD suppression that is achieved experimentally.

ACKNOWLEDGEMENTS

This work was partly funded by the UP System Emerging Interdisciplinary Research Program (OVPA-EIDR-C2-B-02-612-07) and the UP System Enhanced Creative Work and Research Grant (ECWRG 2014-11). This work was supported by the Versatile Instrumentation System for Science Education and Research, and the PCIEERD DOST STAMP (Standards and Testing Automated Modular Platform) Project.

REFERENCES

Eriksen, R., Daria, V. and Gluckstad, J., 2002. Fully dynamic multiple-beam optical tweezers. *Optics Express*, *10*(14), pp.597-602.

Polin, M., Ladavac, K., Lee, S.H., Roichman, Y. and Grier, D., 2005. Optimized holographic optical traps. *Optics Express*, *13*(15), pp.5831-5845.

Palima, D. and Daria, V.R., 2007. Holographic projection of arbitrary light patterns with a suppressed zero-order beam. *Applied optics*, *46*(20), pp.4197-4201.

Nikolenko, V., Watson, B.O., Araya, R., Woodruff, A., Peterka, D.S. and Yuste, R., 2008. SLM Microscopy: scanless two-photon imaging and photostimulation using spatial light modulators. *Frontiers in neural circuits*, *2*, p.5.

Jenness, N.J., Hill, R.T., Hucknall, A., Chilkoti, A. and Clark, R.L., 2010. A versatile diffractive maskless lithography for single-shot and serial microfabrication. *Optics express*, *18*(11), pp.11754-11762.

Hilario, P.L., Villangca, M.J. and Tapang, G., 2014. Independent light fields generated using a phase-only spatial light modulator. *Optics letters*, *39*(7), pp.2036-2039.

Zhu, L. and Wang, J., 2014. Arbitrary manipulation of spatial amplitude and phase using phase-only spatial light modulators. *Scientific reports*, *4*, p.7441.

Dufresne, E.R., Spalding, G.C., Dearing, M.T., Sheets, S.A. and Grier, D.G., 2001. Computer-generated holographic optical tweezer arrays. *Review of Scientific Instruments*, *72*(3), pp.1810-1816.

Melville, H., Milne, G., Spalding, G., Sibbett, W., Dholakia, K. and McGloin, D., 2003. Optical trapping of three-dimensional structures using dynamic holograms. *Optics Express*, *11*(26), pp.3562-3567.

Farsari, M., Huang, S., Birch, P., Claret-Tournier, F., Young, R., Budgett, D., Bradfield, C. and Chatwin, C., 1999. Microfabrication by use of a spatial light modulator in the ultraviolet: experimental results. *Optics letters*, *24*(8), pp.549-550.

Shao, Yonghong, et al. "Addressable multiregional and multifocal multiphoton microscopy based on a spatial light modulator." *Journal of biomedical optics*17.3 (2012): 0305051-0305053.

Fahrbach, F.O., Gurchenkov, V., Alessandri, K., Nassoy, P. and Rohrbach, A., 2013. Light-sheet microscopy in thick media using scanned Bessel beams and two-photon fluorescence excitation. *Optics express*, *21*(11), pp.13824-13839.

Gerchberg, R.W. W. O. Saxton, 1972. A practical algorithm for the determination of phase from image and diffraction plane pictures. *Optik*, *35*, p.237.

Tapang, G. and Saloma, C., 2002. Behavior of the point-spread function in photon-limited confocal microscopy. *Applied optics*, *41*(8), pp.1534-1540.

Ronzitti, E., Guillon, M., de Sars, V. and Emiliani, V., 2012. LCoS nematic SLM characterization and modeling for diffraction efficiency optimization, zero and ghost orders suppression. *Optics express*, *20*(16), pp.17843-17855.

Lizana, A., Moreno, I., Márquez, A., Iemmi, C., Fernández, E., Campos, J. and Yzuel, M.J., 2008. Time fluctuations of the phase modulation in a liquid crystal on silicon display: characterization and effects in diffractive optics.*Optics Express*, *16*(21), pp.16711-16722.

Persson, M., Engström, D. and Goksör, M., 2012. Reducing the effect of pixel crosstalk in phase only spatial light modulators. *Optics express*,*20*(20), pp.22334-22343.

Alagao, M., Go, M., Soriano, M., and Tapang, G., Improving the point spread function of an aberrated 7-mirror segmented reflecting microscope using a spatial light modulator. *Photoptics.* Area 9-Optics. 2016.